## **CONFERENCE PRE-PRINT**

# A SIMULATION STUDY OF PLASMA BREAKDOWN IN THE TOKAMAK ELECTRON CYCLOTRON PRE-IONIZATION PHASE

Jinwoo Gwak Department of Nuclear Engineering, Seoul National University Seoul, Republic of Korea

Min-Gu Yoo General Atomics San Diego, CA 92186-5608, United States of America Email: yoom@fusion.gat.com

Jeongwon Lee Korea Institute of Fusion Energy Daejeon, Republic of Korea

Yeongsun Lee Department of Nuclear Engineering, Seoul National University Nuclear Research Institute for Future Technology and Policy, Seoul National University Seoul, Republic of Korea

Hyun-Tae Kim United Kingdom Atomic Energy Authority, Culham Science Centre Abingdon, OX14 3DB, United Kingdom of Great Britain and Northern Ireland

Yong-Su Na Department of Nuclear Engineering, Seoul National University Seoul, Republic of Korea Email: ysna@snu.ac.kr

### **Abstract**

Early deposition of an electron cyclotron (EC) Gaussian beam in tokamaks can solely pre-ionize neutral gas and lead to plasma breakdown, even prior to the application of significant inductive electric fields. Nonlinear wave trapping under second harmonic resonance provides a finite energy gain to seed electrons beyond the ionization potential, though collisions do not play a role during wave-particle interaction. We present results of EC breakdown simulations by incorporating EC energy gain models into particle simulation code, BREAK (Yoo *et al* 2018 *Nat. Commun.* 9 3523). Mutual agreement is demonstrated with a phenomenological model for the electron impact ionization rate that recasts the classical Townsend framework, leading to a cross-verification of the two approaches. The introduction of a vertical magnetic field as a proxy for the dominant parallel loss establishes a distinct breakdown threshold.

## 1. INTRODUCTION

Injection of high-power electron cyclotron (EC) waves to facilitate tokamak plasma initiation has become a cornerstone of modern start-up scenarios, motivated by the engineering difficulties of purely inductive breakdown and subsequent impurity burn-through in large-scale devices [1–3]. Even prior to the application of a significant loop voltage, a Gaussian wave can solely ionize the plasma, which accelerates or even bypasses the conventional avalanche process, thereby circumventing issues tied to inductive breakdown such as flux consumption and magnetic stray field sensitivities [4–6]. Systematic experimental studies have confirmed its efficacy as an alternative breakdown scenario—even at the second harmonic extra-ordinary (X2) resonance suitable for half-field operation—and have identified key features including a breakdown delay of a few to tens of milliseconds and a minimum power threshold for observable ionization (see e.g. [4–9] and references therein). The important subject

is therefore to establish a predictive understanding of the tokamak microwave breakdown condition, governed by the competition between ionization and loss rate, from which the operational parameter requirements for future devices can be reliably inferred [8].

Achieving this for microwave breakdown, however, remains elusive, as it requires a model that simultaneously couples nonlinear wave-particle interactions [10], avalanche dynamics, and the competing particle loss mechanism. While the key role of nonlinear wave-trapping in the seed electron energy gain for tokamak microwave breakdown is well-established [10–15], prior computational studies have largely focused on the demanding task of modeling the electron multiplication driven by this nonlinear heating, a process they captured by integrating the full electron gyro-orbits [16, 17]. This focus has often left the competing loss term required to establish a breakdown threshold unexplored.

This work presents particle simulations of the X2 microwave tokamak breakdown process with relevant approximations. The electron avalanche dynamics are self-consistently simulated by incorporating the nonlinear EC energy gain model framework [18] into the 2D (R,Z) tokamak breakdown particle-in-cell (PIC) code, BREAK [19–21]. Concurrently, a corresponding ionization rate model for the EC-driven breakdown in tokamaks is constructed by recasting the Townsend theory, providing mutual verification with observed growth rates. The inclusion of a parallel electron loss recovers a distinct breakdown threshold, from which a minimal requirements on operation parameters can be inferred.

The paper is structured as follows: Section 2 details the simulation framework and presents a baseline case; Section 3 benchmarks the ideal ionization rate against a recast Townsend theory; and Section 4 introduces parallel particle loss to determine the breakdown threshold. Finally, section 5 presents summary.

## 2. GENERAL CONSIDERATIONS

## 2.1. Key physical assumptions and EC wave-particle interaction coupling

We focus on the interplay of toroidally asymmetric energy gain from EC wave-particle interactions and the dominant electron-neutral collisions during the avalanche. The background  $H_2$  gas is assumed to be a uniform medium with constant density, allowing the ionization rate to be isolated from neutral screening and depletion effects. A prescribed, radially injected monochromatic X2 Gaussian wave is then introduced, with a polarization consistent with the low plasma frequency limit and propagating perpendicular to the magnetic field,  $B_{\phi}$ . In this rarefied, early-stage regime, collective plasma effects (e.g., Coulomb collisions, space-charge fields [20]) and wave-feedback are neglected.

The EC wave-particle interaction and resultant electron energy gain are encapsulated in the BREAK code via a partitioned framework that applies different models based on the incident electron velocity, as illustrated in figure 1 [18]. For slowly transiting electrons ( $\tau_{\rm flight} \gg \tau_{\rm trap}$ ), the energy gain is treated as a probabilistic jump based on the collisionless adiabatic nonlinear theory [12, 22–24]. Following our recent work [18], we categorize this population into cold electrons (those with zero incident perpendicular energy) and hot electrons (those with low parallel but large perpendicular energy). We employ analytic [10] and semi-analytic models [18] for these two populations, respectively, with corresponding jump probabilities of 100% and 50%; the former is motivated by prior numerical work showing a near-unity probability [25], while the utility of the latter simplification was demonstrated in our recent study [18]. Conversely, for rapidly transiting electrons, the energy gain is calculated by integrating the cyclotron-averaged (secular) equations of motion, which include concurrent collisional effects and are averaged over initial gyro-phases [26].

Collisional processes outside beam region lead to a continuous smearing in phase space, populating the transition region around  $\tau_{\rm flight}/\tau_{\rm trap}\sim \mathcal{O}(1)$ . While a gradual spreading of energy gain is expected for electrons in this regime, however, the contribution of this sub-population to the total energy absorption is considered minor. This suggests that the macroscopic avalanche dynamics are robust against the specific placement of the boundary delineating the adiabatic and secular motion integration models, provided it is of order unity. For this framework, we therefore employ a boundary at  $\tau_{\rm flight}/\tau_{\rm trap}=1$  [27].

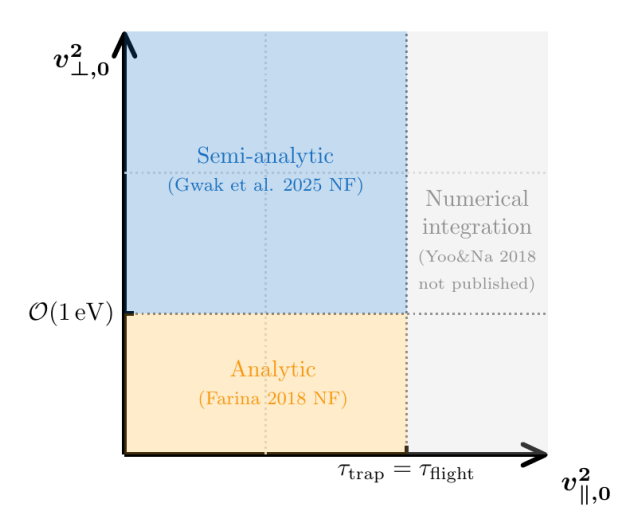


FIG. 1. Application domains of the different energy gain models employed in this work, covering the entire electron phase space. The x- and y-axes are the incident parallel and perpendicular energies, respectively, for an electron entering the beam illumination region.

#### 2.2. Baseline characteristics of the EC-Induced Avalanche

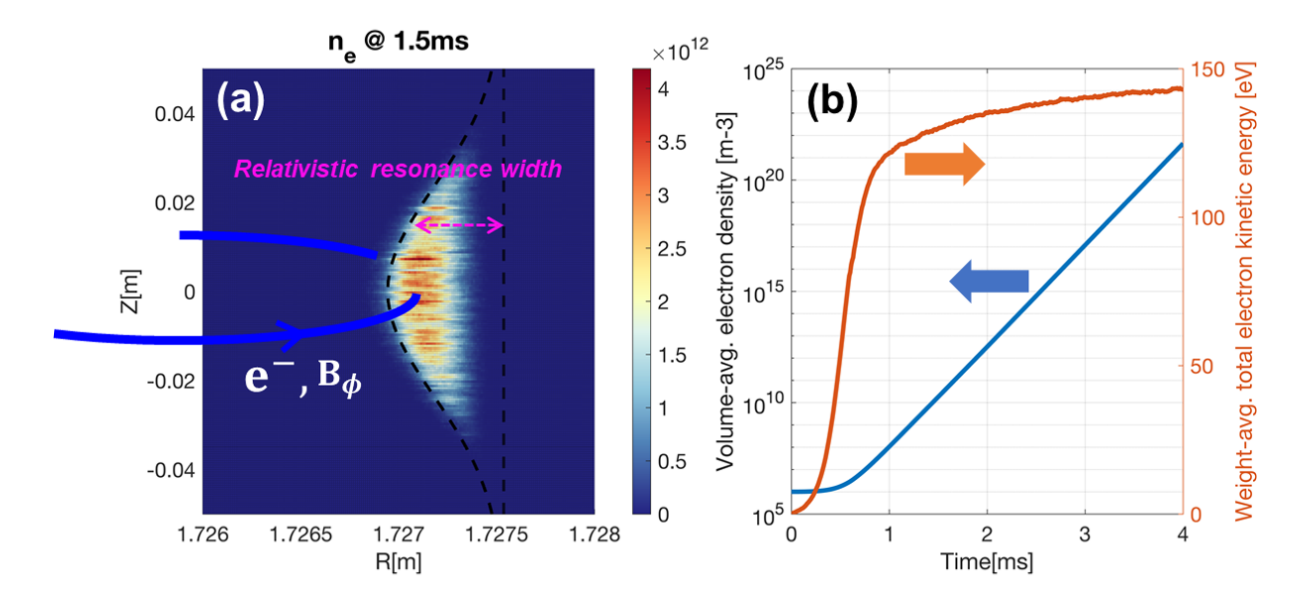


FIG. 2. Results from a particle simulation of electron avalanche dynamics in a pure toroidal magnetic field, where only toroidal transit motion is permitted. (a) Typical two-dimensional (R,Z) electron density distribution. The spatial region corresponding to the resonance width for cold electrons is indicated by the black dashed line [10]. (b) Time evolution of the total electron density and the volume-averaged total kinetic energy.

We first conducted a fiducial simulation of EC-induced electron avalanche. Figure 2(a) shows a time-slice of the spatial electron density distribution for a case with a purely toroidal magnetic field, where charged particles are perfectly confined by suppressing the magnetic drifts to isolate transport effects. The key simulation parameters are as follows: a toroidal field  $B_{\phi} = (-2.4 \times 1.8) R^{-1} \hat{\phi} T$ ; an injected beam power  $P_{\rm inj.} = 0.6 \, \rm MW$  with a radius  $r = 0.033 \, \rm m$  and frequency  $\omega = 2\pi \times 140 \, \rm GHz$ ; an  $H_2$  prefill pressure  $p_{\rm prefill} = 1 \, \rm mPa$ ; and an initial seed plasma (electrons and  $H_2^+$  ions) with a density of  $10^6 \, \rm m^{-3}$  and temperature of  $0.026 \, \rm eV$ . The black dashed lines mark the radial region in the major radius R of the tokamak's cylindrical coordinate system  $(R, \phi, Z)$  where nonlinear trapping occurs for cold electrons. The radial extent, R, of this resonance region is given by:

$$0 < 1 - \frac{\omega}{2\Omega_{ce,0}} \frac{R}{R_0} < \epsilon_M(Z) \tag{1}$$

where the subscript zero indicates values at the machine axis, and  $\epsilon_M(Z) = |e|E(Z)/(m_e\omega c)$  is the normalized beam amplitude exhibiting a Gaussian dependence on the vertical position [10].

It is found that the electron avalanche is strictly confined to the region where the heating of cold electrons occurs exclusively, which is consistent with previous analysis (e.g. see figure 10 in [25]). The time evolution of the volume-averaged density and the weight-averaged total kinetic energy are summarized in Figure 2(b). The mean kinetic energy of high-weight particles rapidly saturates to a value slightly below the mean nonlinear gain at beam axis,  $\epsilon_M m_e c^2 \approx 170~{\rm eV}$ . A sustained exponential growth in density is observed, leading to a breakdown delay of a few milliseconds to surpass  $10^{18}~{\rm m}^{-3}$ —a threshold typically required to create observable ionization in experiments. This delay is shorter than experimental observations [4–9], though of a similar order of magnitude, as is expected from an isolated model that excludes particle loss mechanisms. The saturated energy state itself reflects a steady-state balance in this transport-free system between gains from nonlinear EC interaction and losses from both inelastic collisions and the power dilution from newly created electrons.

## 3. AVALANCHE GROWTH RATE UNDER PERFECT CONFINEMENT

The applicability of the classical Townsend framework to inductive tokamak breakdown is well-founded, largely due to the spatial symmetry of the bulk inductive electric field. However, the intrinsic asymmetries of localized Gaussian wave have so far precluded the development of a similarly rigorous or even phenomenological theory for the macroscopic avalanche growth rate. As most advanced diagnostics oriented toward fusion plasma are infeasible under the relevant parameter range of breakdown, experimental validation of the simulated growth rate also remains elusive. Building on the simulations in the perfectly-confined system from the preceding chapter, we have constructed a phenomenological model that recasts the Townsend framework to interpret the ideal growth rate. The essence of this model lies in substituting the classical framework's parameters with quantities pertinent to resonant electrons; the macroscopic absorption is approximated by the zero-temperature asymptote of the Maxwellian-averaged nonlinear energy gain [18], and a characteristic toroidal transit energy corresponding to 20 eV is adopted, as inferred from the simulation results.

Figure 3 shows the ideal growth rate,  $\gamma_{iz.}$ , from both the simulation and the phenomenological model, depending on the background neutral prefill pressure. Both models indicate that the growth rate increases with pressure, underpinning the experimental observations in part [8]. The agreement is qualitative, and the quantitative deviation is understood to arise from the fact that the PIC simulation accounts for the avalanche of the *entire* electron system—including collisional energy transfer from resonant to non-resonant particles—while the recast model is inherently limited to the avalanche driven solely by resonant electrons. Nevertheless, the consistency between these two disparate approaches—one resolving microscopic particle dynamics and the other employing a macroscopic framework—is noteworthy, as it provides mutual support for both models. The simulation's behavior is corroborated by the established theoretical framework, while the applicability of the Townsend framework to microwave tokamak breakdown is, in turn, supported by the simulation.

## 4. INCLUSION OF PARALLEL LOSS AND BREAKDOWN CONDITION

A central issue in pre-ionization experiments is to interpret the observed requirements on control parameters, such as EC power and prefill pressure, and to reliably extrapolate them to future devices [3, 8]. The threshold nature of this process is fundamentally understood as a competition between the ionization rate and the particle loss rate [28]. While prior semi-empirical models have focused on fitting a net growth rate [16, 17], they often subsumed particle loss into an effective parameter rather than treating it as a direct competitor to the ionization source. A critical consequence of such an approach is its potential failure to predict the existence of control parameter thresholds for observable ionization—a feature that is not only experimentally observed [8,9] but also has a well-established analogue in the minimum inductive electric field of the classical Townsend theory [1]. Building on the distinct dependence of the ideal growth rate on prefill pressure shown in the preceding chapter, we therefore perform an analytical estimation of the breakdown threshold by incorporating a dominant loss channel.

In the tokamak breakdown phase, as in the inductive start-up, the dominant loss channel is parallel transport along magnetic field lines with a finite connection length, created by poloidal stray magnetic fields. We can estimate this loss rate by introducing a small vertical magnetic field ( $B_Z$ ) in our particle simulation as a proxy for experimental stray fields of a comparable magnitude. Figure 4(a) juxtaposes the ideal ionization rate (figure 3) with the estimated loss rate,  $\nu_{\rm loss}$ , for several values of  $B_Z$ , where  $\nu_{\rm loss} = (2\langle W_\parallel \rangle/m_e)^{1/2}(B_Z/aB_{\phi,\rm res})$ . For

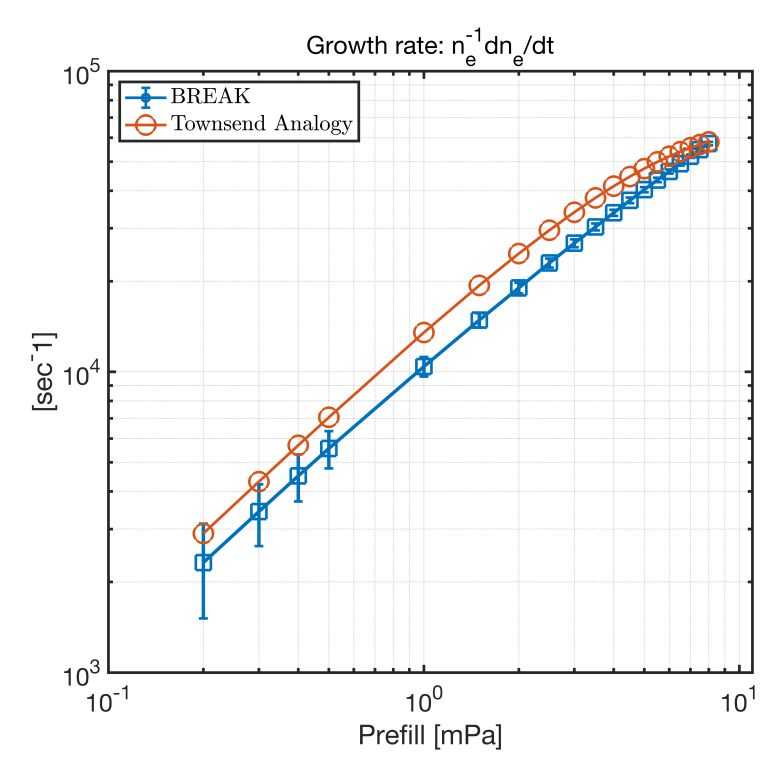


FIG. 3. Exponential density growth rate from avalanche simulation and recast Townsend model. Identical settings of figure 2 are used, excepting prefill pressure.

this estimation, we adopt a mean parallel kinetic energy of  $20~{\rm eV}$ , again inferred from simulations, and a poloidal distance to travel of  $a=1.2~{\rm m}$ , characteristic of a KSTAR-like vacuum vessel. This simple balance model allows for the identification of distinct cases, marked by circles and triangles, where the breakdown is predicted to either succeed ( $\gamma_{\rm iz.} > \nu_{\rm loss}$ ) or fail ( $\gamma_{\rm iz.} < \nu_{\rm loss}$ ), respectively.

To validate these predictions, we then conducted simulations for these selected cases under their corresponding magnetic configurations, now incorporating particle transport effects, including parallel streaming and magnetic drift motions, within a numerical domain bounded by  $Z=\pm 1.2~\mathrm{m}$ . The time evolution of the volume-averaged electron densities from these simulations, shown in figure 4(b), directly confirms the predictions from the simplified model. A sustained, exponential growth in density is observed for the success cases (1) and (2), in stark contrast to the failure cases (3) and (4), where the initial electron multiplication halts without igniting a self-sustaining chain reaction. This demonstrates that the breakdown threshold in tokamak EC pre-ionization phase can be interpreted and theoretically predicted by a straightforward balance between the ionization rate and an analytically tractable parallel loss model, a conclusion that is evidently corroborated by the full microscopic dynamics resolved in the high-fidelity particle simulation.

## 5. SUMMARY

In summary, we establish a self-consistent model of the X2 microwave tokamak breakdown. By incorporating the nonlinear EC energy gain model framework [18] into the particle-in-cell code BREAK, a verifiable, first-principles description of the avalanche dynamics has been achieved. In an isolated toroidal-slab geometry, simulations with perfect confinement yield a growth rate comparable to a recast Townsend theory, demonstrating the qualitative trend of an enhanced ionization rate with increasing prefill pressure, which underpin previous experimental observations. The competition between the verified ionization rate and the dominant parallel loss mechanism establishes a distinct breakdown threshold, the robustness of which was corroborated in simulations that incorporated parallel streaming, magnetic drift motions, and a small vertical magnetic field acting as a proxy for experimental stray fields of a comparable magnitude. Future work will focus on a systematic comparison of the predicted power thresholds with values reported from various experimental devices [8, 9].

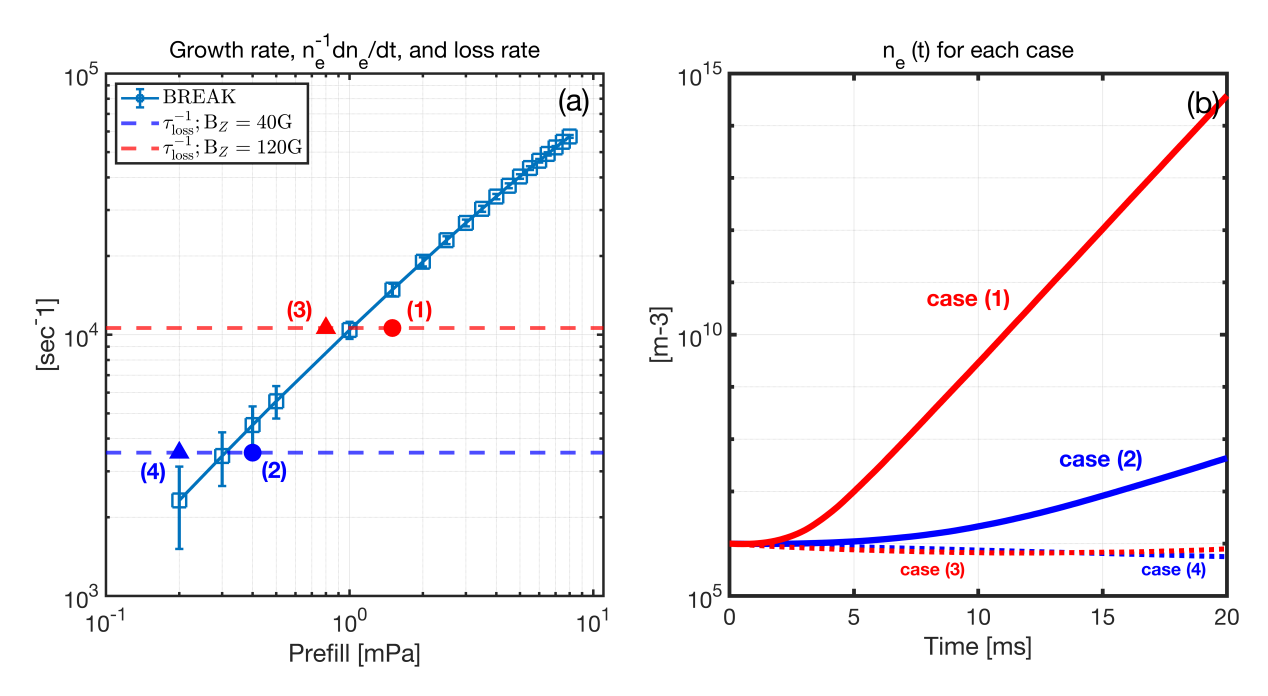


FIG. 4. Breakdown threshold determined by the balance between the ionization growth rate and the particle loss rate. (a) Comparison of the ideal ionization rate (figure. 3) with the expected parallel loss rate for different conditions of  $B_Z$ . (b) Time evolution of the electron density from simulations including  $B_Z$  and drift motions, performed for each of the corresponding conditions shown on the (a).

#### ACKNOWLEDGEMENTS

This work was supported by the National R&D Program through the National Research Foundation of Korea (NRF) funded by the Korea government (Ministry of Science and ICT) (NRF-2021M1A7A4091135). This research has also been supported by R&D Program of "High Performance Tokamak Plasma Research & Development (code No EN2501)" through the Korea Institute of Fusion Energy (KFE) funded by the Government funds, Republic of Korea.

## REFERENCES

- [1] LLOYD, B. et al., Low voltage Ohmic and electron cyclotron heating assisted startup in DIII-D, Nucl. Fusion **31** (1991) 2031.
- [2] GRIBOV, Y. et al., Chapter 8: Plasma operation and control, Nucl. Fusion 47 (2007) S385.
- [3] De Vries, P. C. and GRIBOV, Y., ITER breakdown and plasma initiation revisited, Nucl. Fusion **59** (2019) 096043.
- [4] KAJIWARA, K. et al., Electron cyclotron heating assisted startup in JT-60U, Nucl. Fusion 45 (2005) 694.
- [5] JACKSON, G. L., DEGRASSIE, J. S., MOELLER, C. P., and PRATER, R., Second harmonic electron cyclotron pre-ionization in the DIII-D tokamak, Nucl. Fusion 47 (2007) 257.
- [6] BAE, Y. et al., ECH pre-ionization and assisted startup in the fully superconducting KSTAR tokamak using second harmonic, Nucl. Fusion **49** (2008) 022001.
- [7] STOBER, J. et al., ECRH-assisted plasma start-up with toroidally inclined launch: multi-machine comparison and perspectives for ITER, Nucl. Fusion **51** (2011) 083031.
- [8] SINHA, J. et al., Studies of EC pre-ionization in DIII-D to support development of ITER plasma initiation, Nucl. Fusion **62** (2022) 066013.
- [9] ZHANG, J. et al., Experimental study of electron cyclotron heating assisted start-up on J-TEXT, Nucl. Fusion **63** (2023) 076028.

- [10] FARINA, D., Nonlinear collisionless electron cyclotron interaction in the pre-ionisation stage, Nucl. Fusion **58** (2018) 066012.
- [11] SEOL, J., PARK, B., KIM, S., KIM, J., and NA, Y.-S., Electron cyclotron heating during ECRH-assisted pre-ionization in a tokamak, Nucl. Fusion **50** (2010) 105008.
- [12] SUVOROV, E. V. and TOKMAN, M. D., Generation of accelerated electrons during cyclotron heating of plasmas, Sov. J. Plasma Phys. **14** (1988) 557.
- [13] SUVOROV, E. V. and TOKMAN, M. D., Theory of microwave breakdown of low-density gas at electron cyclotron resonance in magnetic mirror systems, Sov. J. Plasma Phys. 15 (1989) 540.
- [14] CARTER, M., BATCHELOR, D., and ENGLAND, A., Second harmonic electron cyclotron breakdown in stellarators, Nucl. Fusion 27 (1987) 985.
- [15] ERCKMANN, V. and GASPARINO, U., Electron cyclotron resonance heating and current drive in toroidal fusion plasmas, Plasma Phys. and Control. Fusion **36** (1994) 1869.
- [16] PAPAGIANNIS, P. C., ANASTASSIOU, G. E., HIZANIDIS, K., and RAM, A. K., Physically based modelling of ec pre-ionization and assisted breakdown under iter-like constraints, in 48th EPS Conference on Plasma Physics, volume 46A of Europhysics Conference Abstracts, Maastricht, Netherlands, 2022, P5a.109.
- [17] PAPAGIANNIS, P. C., TSIRONIS, C., HIZANIDIS, K., and ANASTASSIOU, G. E., Breakdown time estimation for ec-assisted start-up in tokamaks, in *20th European Fusion Theory Conference*, Padova, Italy, 2023, Poster presentation, P2.25.
- [18] GWAK, J. et al., Modelling of electron cyclotron energy gain in the tokamak pre-ionization phase, Nucl. Fusion **65** (2025) 056038.
- [19] YOO, M.-G., LEE, J., KIM, Y.-G., and NA, Y.-S., Development of 2D implicit particle simulation code for ohmic breakdown physics in a tokamak, Comput. Phys. Commun. **221** (2017) 143.
- [20] YOO, M.-G. et al., Evidence of a turbulent ExB mixing avalanche mechanism of gas breakdown in strongly magnetized systems, Nat. Commun. 9 (2018) 3523.
- [21] YOO, M.-G. and NA, Y.-S., Understanding the electromagnetic topology during the ohmic breakdown in tokamaks considering self-generated electric fields, Plasma Phys. and Control. Fusion **64** (2022) 054008.
- [22] NEVINS, W. M., ROGNLIEN, T. D., and COHEN, B. I., Nonlinear absorption of intense microwave pulses, Phys. Rev. Lett. **59** (1987) 60.
- [23] KOTEL'NIKOV, I. A. and STUPAKOV, G. V., Nonlinear effects in electron cyclotron plasma heating, Phys. Fluids B 2 (1990) 881.
- [24] FARINA, D. and POZZOLI, R., Nonlinear electron-cyclotron power absorption, Phys. Fluids B 3 (1991) 1570.
- [25] FARINA, D., Electron Cyclotron collisionless interaction during EC-assisted tokamak start-up, EPJ Web Conf. **203** (2019) 01001.
- [26] YOO, M.-G. and NA, Y.-S., Feasibility of 3rd harmonic electron cyclotron heating for the pre-ionization, 2018, In *ITPA IOS-TG Meeting*. This unpublished presentation was conducted on the International Tokamak Physics Activity (ITPA) Integrated Operation Scenarios Topical Group (IOS-TG) meeting which was held at, NFRI, Daejeon, Republic of Korea.
- [27] JOHANSSON, C. A. and ALEYNIKOV, P., Electron cyclotron resonance during plasma initiation, J. Plasma Phys. **90** (2024) 905900103.
- [28] RAIZER, Y. P., Gas discharge physics, Springer, Berlin, New York, 1991.